



Published in final edited form as:

Anal Chem. 2013 July 2; 85(13): 6312–6318. doi:10.1021/ac400575u.

Phosphorescent nanosensors for *in vivo* tracking of histamine levels

Kevin J. Cash¹ and Heather A. Clark^{1,*}

¹Department of Pharmaceutical Sciences, Northeastern University, Boston, MA, 02115, USA

Abstract

Continuously tracking bio-analytes *in vivo* will enable clinicians and researchers to profile normal physiology and monitor diseased states. Current *in vivo* monitoring system designs are limited by invasive implantation procedures and bio-fouling, limiting the utility of these tools for obtaining physiologic data. In this work, we demonstrate the first success in optically tracking histamine levels *in vivo* using a modular, injectable sensing platform based on a diamine oxidase and a phosphorescent oxygen nanosensor. Our new approach increases the range of measureable analytes by combining an enzymatic recognition element with a reversible nanosensor capable of measuring the effects of enzymatic activity. We use these enzyme nanosensors (EnzNS) to monitor the *in vivo* histamine dynamics as the concentration rapidly increases and decreases due to administration and clearance. The EnzNS system measured kinetics that match those reported from *ex vivo* measurements. This work establishes a modular approach to *in vivo* nanosensor design for measuring a broad range of potential target analytes. Simply replacing the recognition enzyme, or both the enzyme and nanosensor, can produce a new sensor system capable of measuring a wide range of specific analytical targets *in vivo*.

Keywords

Diagnostic; Biosensor; Fluorescence; Histamine; Optode

Continuously monitoring *in vivo* analyte concentrations would benefit a wide range of applications such as pharmacokinetic profiling of novel drugs or drug candidates and tracking biomarker concentrations during disease progression or treatment. Current approaches rely on blood sampling followed by offline analysis. This process, while effective in some cases, poses limitations when applied to common research models such as mice due to limitations on the amount and frequency of blood sampling. Research during the past several decades has greatly improved *in vitro* and *in vivo* analysis through the

*Corresponding Author Heather A. Clark, PhD, Associate Professor, Department of Pharmaceutical Sciences, Northeastern University, 206 TF, 360 Huntington Ave, Boston, MA 02115, (617) 373-3091, h.clark@neu.edu, www.neu.edu/nanosensors.

ASSOCIATED CONTENT

Additional *in vitro* characterization, experimental methods, and expanded *in vivo* data are presented in the supporting information. This material is available free of charge via the Internet at <http://pubs.acs.org>

Author Contributions

The manuscript was written through contributions of all authors. All authors have given approval to the final version of the manuscript.

development of enzymatic biosensors^{1, 2}. The range of *in vivo* sensors available for either basic research or clinical diagnostics has continually grown, although the best developed are those for glucose. The earliest enzymatic biosensor design³ paired the enzyme, glucose oxidase, with a pH electrode. In this approach, glucose oxidase catalytically oxidizes glucose into gluconic acid, which lowers the pH, and the measured pH change correlates to glucose concentration. More modern approaches for glucose detection rely on electron transfer mediators rather than oxygen consumption or pH detection, and this sensor family has enjoyed success in the form of the handheld glucometer as well as a wide variety of laboratory and clinical diagnostic assays.

Enzyme-based sensors can recognize a broad range of target analytes with high recognition specificity, but enzyme based biosensors, including those for glucose, are still primarily based on electrochemical sensors⁴. Although these electrode-based enzymatic biosensors perform well for *in vitro* measurements, several key difficulties prevent them from achieving widespread *in vivo* use. Electrode-based sensors are inherently invasive, and their transdermal electrodes pose a risk for implant site infection⁵. Additionally, the foreign body response encapsulates the implanted electrode, effectively isolating the device from the biological fluid it is intended to sample⁵. Consequently, electrode-based sensors currently must be re-implanted every week to maintain an adequate signal, and this procedure is not only a major inconvenience for the patient but is also an additional opportunity for infections⁶.

Sensors that use optical interrogation can minimize the invasiveness of continuous measurement systems by eliminating any transdermal components. Small-molecule, optically-dynamic recognition elements are appealing options, and although a few examples such as boronic acid derivatives can measure *in vivo* glucose concentrations⁷⁻⁹, such systems are developed ad-hoc. However, enzyme-based biosensors are modular and generalizable for any enzyme that consumes, produces, or alters pH and/or oxygen by pairing them with pH or oxygen-sensing optical systems. This approach is well-developed for monitoring glucose (see reviews¹⁰ and nanotechnology-based approaches¹¹⁻¹³), but this technique's broad effectiveness still needs to be demonstrated *in vivo* for other small molecule analytes.

Optode based nanosensors are a modular family of sensors that are capable of continuously monitoring *in vivo* physiological parameters such as oxygen and pH. Optode nanosensors are composed of a hydrophobic, plasticized polymer core that contains hydrophobic sensor components and a polyethylene glycol (PEG) coating for solubility and biocompatibility. The sensors are approximately 100 nm in diameter, and specific nanosensor formulations that emit a reversible, concentration-dependent fluorescent signal for specific ions (Na⁺) or glucose *in vivo* are already published^{9, 14, 15}. The nanosensors are small enough for a simple subcutaneous injection, and their transdermal fluorescent signal is measurable with commercially-available animal imaging systems. Incorporating enzymes for recognition elements, as has been done for other optical sensor techniques^{1, 16, 17}, would vastly expand the range of detectable biological analytes using this platform and constitute a significant advance in the field of non-invasive continuous analyte monitoring primarily through removing the electrode and associated risk. While biocompatibility and toxicity research is

still necessary for safely designing implantable nanomaterials, and is still an ongoing field of research¹⁸, surface coatings with PEG domains can minimize protein fouling and safely prolong nanoparticle clearance¹⁹ and the use of biocompatible polymers (e.g. PLGA) will likely minimize risks²⁰. Additionally, some of the components used in both approaches, namely the enzymatic recognition elements, are already approved in some human applications (e.g. glucose oxidase sensors²). The approach coupling enzymatic recognition with optode based nanosensors enables straightforward, less invasive analyte monitoring when compared with electrode-based approaches.

Histamine is an important biochemical intermediary in allergy and inflammation²¹, neurotransmission²², gastric disorders, chronic myelogenous leukemia^{23, 24}, and bacterial signaling²⁵. Histamine measurements predominantly rely on discrete microdialysis or blood sampling followed by offline measurements such as HPLC^{26, 27}. Although this approach functions adequately for some experiments, it does impose limitations on the ability to monitor histamine concentrations in real time or in the absence of clinical laboratories for analysis, and suffers some of the same implantation drawbacks of electrode sensors²⁸. *In vivo* histamine concentrations vary over a wide range, from a resting plasma concentration as low as 4 nM²⁹ to 240 μ M in diseased states²⁴ and as high as hundreds of mM inside mast cells³⁰. A system capable of continuously monitoring systemic histamine levels would help delineate event progression in basic biological processes such as allergic response and neurobiology as well as the improved developmental testing of drugs targeting the histamine pathway.

In this paper we couple together the approach of enzyme recognition biosensors with optical nanosensors to enable continuous histamine tracking *in vivo* without the need for blood sampling. To validate the system, we measured and modeled histamine pharmacokinetics and compared them with established values from offline measurements. The nanosensor-based measurements matched established pharmacokinetic properties for *in vivo* histamine clearance without the time, expense, or difficulty of previously-used offline methods. More importantly, the histamine sensor shows that a modular enzyme-nanosensor design is capable of continuously tracking small biomolecules *in vivo*. Through the use of alternate enzymes and nanosensors, a suite of sensors is under development for additional targets including acetylcholine and dopamine for *in vivo* and *in vitro* applications.

Experimental

Materials

Poly(vinyl chloride) (PVC), Bis(2-ethylhexyl) sebacate (DOS), tetrahydrofuran (THF), dichloromethane, Tris(4,7-diphenyl-1,10-phenanthroline)ruthenium(II) dichloride complex, and histamine dihydrochloride were purchased from Sigma Aldrich (St. Louis, MO). 5,10,15,20-Tetrakis(pentafluorophenyl)-21H,23H-porphine, platinum(II) (PtTPFP) was purchased from Frontier Scientific (Logan, UT).

1,2-distearoyl-sn-glycero-3-phosphoethanolamine-N-[methoxy(polyethylene glycol)-550] ammonium salt in chloroform (PEG-lipid) was purchased from Avanti Polar Lipids (Alabaster, AL). Diamine oxidase (DAO, 35 IU/mL) was purchased from Bio-Research

Products Inc. (North Liberty, IA). Spectra/Por[®] *In Vivo* Microdialysis Hollow Fibers (13 kDa MWCO, 200 μ m inner diameter) was purchased from Spectrum Laboratories, Inc. (Rancho Dominguez, CA). Epoxy (H2Hold) was purchased from ITW Performance Polymers (Riviera Beach, FL) and phosphate buffered saline (PBS, pH=7.4) was purchased from Life Technologies (Grand Island, NY).

Animal Research

All animal experiments were approved by the institutional animal care and usage committee (IACUC) of Northeastern University as well as the US Army Medical Research and Materiel Command (USAMRMC) Animal Care and Use Review Office (ACURO). The mice used in this research were male CD-1 Nude mice from Charles River (Wilmington MA). All experiments were carried out at Northeastern University.

Nanosensor Fabrication

Oxygen nanosensors (O₂NS) were fabricated using methods previously reported for ion sensitive nanosensors^{14, 31}. In brief, this process starts with formulation of an optode dissolved in 500 μ L THF comprising 30 mg PVC, 60 μ L DOS, and 10.5 mg PtTPFP. In a scintillation vial, 2 mg of PEG-lipid was dried and then resuspended in 5 mL PBS with a probe tip sonicator for 30 seconds at 20% intensity (Branson, Danbury CT). 50 μ L of the optode solution was diluted with 50 μ L of dichloromethane, and the mixture was added to the PBS/PEG-lipid solution while under probe tip sonication (3 minutes, 20% intensity). The nanosensor solution was filtered with 0.22 μ m syringe filter to remove excess polymer (Pall Corporation, Port Washington, NY). Nanosensors were sized with a Brookhaven 90Plus (Holtsville, NY) and had an effective diameter of approximately 100 nm. A rough estimate of particle concentration, based on Nanoparticle Tracking Analysis (NTA, Nanosight, Amesbury, UK) of a similar nanosensor preparation yields a concentration of $\sim 1.5 \times 10^{12}$ particles/mL. EnzNS solution was prepared by mixing oxygen nanosensors with DAO solution (35 IU/mL) in a 1:1 volume ratio. Final concentrations were $\sim 0.75 \times 10^{12}$ particles/mL and 17.5 IU/mL DAO.

In vitro characterization

EnzNS solution was loaded into microdialysis tubing via capillary action. The ends of the microdialysis tube were sealed with epoxy, and adhered to the bottom of a culture dish with an optical glass bottom. The setup was submerged in PBS for 1 hour to allow the epoxy to harden. All images were taken using a Zeiss confocal microscope (LSM 700) using 405 nm excitation and capturing emission above 612 nm using a 10X air objective. The histamine concentration was increased by addition of histamine stock solution (100 mM). Image analysis was performed using ImageJ. Intensity values were extracted from a three region of interest within the dialysis tubing which were averaged together. Example images from calibration are in Figure S2. Sensor affinity was determined with a dose response curve using OriginPro software (OriginLab, Northampton, MA) and the Hill1 fit. The limit of detection was determined as the concentration where the signal from the fit would be above 3 standard deviations from the blank signal. Reversibility cycling was conducted using a modified system with the microdialysis tubing affixed to a 20 mm glass coverslip loaded

into a perfusion system on the microscope. Solutions of either 0 mM or 10 mM histamine were alternately filled into the system by gravity for a total of five cycles. This was repeated with three separate dialysis tubes in separate experiments. One region of interest was extracted from each experiment and these were averaged together. Figure 3 shows the error bars for every five data points, the full dataset is presented in Figure S1A.

Additional *in vitro* characterization, detailed in the supplementary information, including photobleaching (Figure S1), batch-to-batch variability (Figure S4), enzyme concentration tuning (Figure S3), as well as accompanying methods.

***In vivo* studies**

All *in vivo* studies were conducted using a Lumina II *in vivo* imaging system (IVIS) from Caliper Life Sciences (Hopkinton, MA). A customized light source was used for excitation of the nanosensors built from 4 high intensity LEDs emitting at 395 nm (Newark Electronics, Chicago, IL) powered by a 9V battery. The IVIS was used in bioluminescence mode (no excitation light from the imager) with a 640 nm emission filter (20 nm bandpass) and 4 second exposure.

The O₂NS were concentrated approximately 10-fold for *in vivo* experiments using Amicon Ultra centrifugal filters (0.5 mL volume, 10 kDa MWCO, Millipore Corporation, Billerica, MA). EnzNS solutions were prepared using concentrated O₂NS nanosensors (25 μL, ~10¹³ particles) and DAO (50 μL, 1.75IU). Final concentrations were 1.3 × 10¹⁴ particles/mL and 23 IU/mL DAO. A higher amount of nanoparticles was utilized to enable transdermal phosphorescence to be visible. As a control, O₂NS injections were made with concentrated nanosensors (25 μL) diluted with 50 μL of PBS. This control serves to measure changes in oxygen levels resulting from biological effects of histamine after injection (e.g. altered metabolism or optical changes in tissue absorbance), and is necessary to enable specifically tracking histamine rather than a combination of histamine and oxygen changes. Mice were weighed, anesthetized with isoflurane (2% isoflurane, 98% oxygen), and placed in the IVIS imager. Two intradermal 30 μL injections of nanosensors were made along the midline of the back. EnzNS was injected posterior to O₂NS. After injection the animals are imaged every 30 seconds for 30 minutes. After that, one mouse was administered 75 mg/kg histamine in PBS (i.p.) while the other mouse was administered PBS of a matching volume. The mice were imaged for an additional 45 minutes to 1 hour. All animals were sacrificed after the end of the experiment. Three separate experiments were performed with new mice and fresh batches of nanosensor solution. Sample images and timecourse data from all experiments are presented in the supplementary information.

For data analysis, a region of interest encompassing the injection area was selected and intensity was recorded. Each intensity value was normalized to the same spot at the first time point after injection of histamine. The difference in normalized signals between the EnzNS and O₂NS was calculated for each mouse. This data was also averaged together across all three experiments using linear interpolation to align time and intensity points before averaging. Raw, normalized and averaged data is presented in the supplementary information. The average data was then fit to a single compartment open model: Equation(1)

$$I = A * \frac{k_a}{k_a - k_e} * [e^{-k_e * (t - t_{lag})} - e^{-k_a * (t - t_{lag})}] \quad (1)$$

Where I is the normalized phosphorescence intensity difference, A is a scaling parameter, k_a and k_e are the absorption and elimination rate constants and t_{lag} is the lag time. The parameters k_a , k_e , and t_{lag} were fit using the method of residuals and A was fit using least squares minimization for plotting purposes.

Results and Discussion

The modular platform for continuous optical biomolecule monitoring uses an enzymatic recognition element and phosphorescent nanosensors. To translate the approach established with glucose oxidase-based electrochemical sensors, we selected an enzyme, diamine oxidase (DAO), which consumes oxygen when it converts histamine into ammonia and imidazole-4-acetaldehyde. When oxygen levels drop near active DAO, oxygen-responsive nanosensors (O₂NS) increase their phosphorescence (Figure 1). The enzyme nanosensor platform (EnzNS) combining O₂NS with DAO detected histamine in both *in vitro* and *in vivo* experiments.

The O₂NS used in this platform are PEG coated plasticized polymer nanoparticles formed through a well-established nanoemulsion technique.^{14, 32} The oxygen responsive element in these sensors is Pt(II) meso-Tetra(pentafluorophenyl)porphine^{12, 33, 34} (PtTPFPP), a hydrophobic platinum porphyrin dye which has a reversible, oxygen-dependent phosphorescent signal, and a ~250 nm Stokes shift, minimizing potential interference from tissue autofluorescence *in vivo*. When O₂NS come into contact with oxygen, the oxygen quenches nanosensor emission, and the nanosensors recover their phosphorescence once oxygen is removed from the environment. To make O₂NS sensitive to histamine, the sensor solution was mixed with a diamine oxidase (DAO) solution to form the EnzNS. In the absence of histamine, an air-saturated EnzNS solution emitted a low phosphorescent signal, indicative of oxygen-induced quenching (Figure 2). Upon addition of histamine, DAO rapidly consumes oxygen ($t_{95\%} = 2.2$ min, limited by mixing system) from the nanosensors, increasing the emission from the EnzNS.

For longitudinal *in vivo* studies, EnzNS must change their phosphorescence in a dose-dependent and reversible manner as histamine levels fluctuate. We demonstrated that EnzNS are reversible by encapsulating EnzNS in microdialysis tubing, washing through several cycles of histamine solutions or histamine-free buffer, and measuring the phosphorescence with a confocal microscope. The EnzNS cannot diffuse across the tube walls, but small molecules such as histamine and oxygen can easily diffuse across the tube wall. Through 5 wash cycles and nearly 75 minutes of imaging, EnzNS reversed and settled to steady-state phosphorescence intensities at each cycle (Figure 3). Although the continuous laser excitation on the confocal microscope induced some photobleaching, the weaker light source used for *in vivo* experimentation did not cause a discernible loss of signal (Figure S1) and without continuous excitation no decrease was seen between sequential histamine solutions (Figure S1). *In vivo*, the vasculature will continuously supply oxygen to the

nanosensors, ensuring that in the absence of oxygen-consuming enzymatic activity, EnzNS will reliably return to a quenched state. Furthermore, the EnzNS dose-response behavior in response to histamine solutions ranging from 1 to 50 mM, fit the Hill binding model well (Figure 4) with a K_d of 3.4 mM and a lower limit of detection of 1.1 mM.

In vivo testing is a common failure point for sensing platforms because proteins may adsorb and foul the sensor, similar biomolecules may produce false positive signals, and normal oxygen fluctuations may mask the sensor's response. For *in vivo* tests, a whole animal imaging system continuously measured the EnzNS phosphorescence in response to changes in systemic histamine. Anesthetized mice received two injections along the centerline of their back; one site for EnzNS and one site for enzyme-free O₂NS. The O₂NS measured systemic oxygen and accounted for any changes in blood oxygenation or skin optical density as a result of the biological effects of histamine. By analyzing phosphorescent dynamics from both spots, an accurate histamine measurement is possible even with concurrent changes resulting from biological effects of histamine.

When the mice received an intraperitoneal histamine injection, the EnzNS implantation site phosphorescence increased by a factor of 2.1 as it responded to histamine (Figure 5, left mouse, lower spot). This increase is below the maximal signal change, indicating a local concentration maximum below 10 mM histamine. The O₂NS implantation site (upper spot) also increased, although the increase was only ~25% as large as the increase from the EnzNS spot. For control mice, who received saline rather than histamine, neither the EnzNS nor the O₂NS injection spots changed throughout the course of the experiment. Figure 5 shows a normalized intensity plot that corrects for the effects of increased oxygen, measured by the O₂NS, showing a clear difference between the control mouse and the histamine mouse that peaks after 12 minutes. After approximately 30 minutes, the EnzNS returned to basal phosphorescence and the two signals from control (saline) and test (histamine) mice were equal (Figure 5).

This kinetic profile agrees with off-line measurement studies that have documented rapid rates for histamine clearance^{35–37}. Running this experiment in triplicate demonstrated the reproducibility for detecting histamine using this approach. All three experiments showed similar response kinetics (see supporting information Figures S6–S8), with biological variation likely accounting for differences. Averaged data from the three experiments fit into a single compartment open model for pharmacokinetics (Equation (1), described in the methods) indicating an approximate absorption half-life of 2.8 minutes and an elimination half-life of 7.6 minutes (Figure 6). Other studies that measured histamine in humans using offline techniques yield elimination half-lives ranging from 4 minutes to 18 minutes^{35, 36, 38}, indicating that the EnzNS system accurately tracked histamine levels as it was cleared from the mice.

Traditional *in vivo* bio-analytical measurement systems have relied on electrochemical detection due to the robust and modular nature of enzyme recognition elements and the sensitivity of electrochemical measurement systems. These systems are undeniably useful for *ex vivo* measurements, but several factors will continue to confound their *in vivo* effectiveness. Primarily, electrode implantation produces local inflammation and induces a

foreign body response with the eventual fate of fibrous capsule formation³⁹. The fibrous capsule limits mass transfer near the electrode, changing measurement profiles, and every new electrode implantation introduces a new potential infection site. Although advances in wireless communications^{5, 40} and supporting electronics may reduce the risk for infection, the foreign body response will still lead to capsule formation and performance loss in signal fidelity.

Nanoparticles implanted by subcutaneous injections minimize the complications from infection risk and capsule formation, and the EnzNS nanoparticles are coated with poly(ethylene glycol) (PEG) to minimize protein fouling¹⁹. This coating allows the nanosensors to provide a continuous signal with minimal side effects. Continuous physiological monitoring is extremely beneficial for longitudinal analyte monitoring in patients with chronic conditions such as diabetes or renal failure as well as in laboratory research. This monitoring is especially valuable for experiments using transgenic mouse models where the number of potential blood samples is limited and the cost per animal is very high, which precludes high temporal resolution for tracking analyte concentrations. In a clinical application, a patient would receive a tattoo-like subdermal injection with a spatially-multiplexed pattern so that each spot would monitor one of several analytes important to maintaining a positive prognosis.

One of the biggest advantages of this approach is the modular nature of the combination of nanosensor and enzyme. Previous optode-based nanosensor formulations relied on the range of available ionophores or boronic acids as recognition elements limits. Until now, those nanosensors were limited in the breadth of potential analytes by the available recognition elements. Here, those same nanosensors detected an enzyme's activity, making the resulting optical signal specifically responsive to the enzyme's target substrate. Now the breadth of target analytes can include many more molecules due to the specific recognition capabilities intrinsic to enzymes. This work focused on histamine, an important biomolecule to allergies and anaphylaxis, but this modular platform enables straightforward application to monitor other biologically important small molecules such as lactate, creatinine and urea. Any of these designs are achievable by replacing diamine oxidase enzyme with an oxidase enzyme for the desired target (Figure S5 demonstrates this approach with glucose and glucose oxidase). Moreover, if an oxidase enzyme is unavailable or ineffective for a desired target, the platform can support a pair of two complimentary enzymes along with the oxygen nanosensors. In such a case, a suitable primary enzyme to the target analyte would be coupled with a secondary oxidase enzyme that targets a breakdown product or cosubstrate from the primary reaction. Nanosensors can be fabricated for a wide range of products to measure based on commercially-available ionophores including ammonium, nitrate, carbonate or pH. This is the first work to demonstrate *in vivo* the principle of enzyme coupled optical nanosensors for histamine detection, and to tune the nanosensors to match their dynamic range to physiological levels for *in vivo* detection.

Looking forward to long-term physiologic monitoring, several challenges stand on the horizon. Continuously tracking *in situ* histamine levels, or those of any analyte, requires that the sensor phosphorescence and response change only negligibly over the course of tracking. Nanosensors and enzymes are both sufficiently small to diffuse away from the injection site

as well as from each other. Although the nanosensors used in this work tracked histamine levels *in vivo* for long enough to observe a return to basal levels, future work will require the sensor system to stay at the injection site for extended lengths of time. Rather than using spherical sensors as with this work, high aspect ratio sensors show significantly slower diffusion rates and keep sensors near the injection site longer⁴¹. Directly conjugating the enzyme to the sensor surface or coencapsulating the enzyme and nanosensor will keep the enzyme and nanosensor from diffusing away from each other, keeping the assembly functional for a longer period of time.

The other step needed for future *in vivo* tracking is to improve the sensitivity of the nanosensors. Many important biomolecules have substantially lower physiological concentrations than the mM levels in this study, and working in the nanomolar or low micromolar range would make detection of targets such as cortisol and other hormones feasible. Direct conjugation of the nanosensor and enzyme, in addition to minimizing diffusion of the components, may also increase the sensitivity of the sensor system through more localized oxygen depletion which will in turn lower the minimal detection limit. The sensor response to oxygen levels can also be modulated through the choice of alternate dyes¹² or polymers⁴². Another important step towards longitudinal monitoring and improved sensitivity will be the incorporation of a reference fluorophore that is not sensitive to oxygen concentrations, which will enable ratiometric measurements. The ratio of the signal from the two dyes will change with oxygen, or in this case histamine, concentrations, but will not depend on sensor concentration as the current approach does. The current approach tracks changes in histamine levels, but the use of ratiometric measurement opens up the possibility of absolute quantification of histamine concentrations *in vivo*. The amount of enzyme utilized relative to the oxygen resupply *in vivo* also contributes to the platform's sensitivity, and varying that ratio is an auxiliary factor to realize a highly sensitive bio-analytical sensor.

Conclusions

In summary, we produced an optical, enzyme based nanosensor system to monitor histamine *in vivo*. The EnzNS platform combined enzymatic biorecognition by diamine oxidase with oxygen sensitive nanosensors that produce a phosphorescent signal visible through the mouse's skin. A dose-response calibration curve and time-course imaging experiments showed that EnzNS are reversible and sensitive in a physiologically-relevant concentration range. We then were able to continuously monitor systemic histamine concentrations in live mice, observing a phosphorescent increase from the histamine dose and then return to normal levels as histamine cleared the mice. Measurements based on EnzNS phosphorescence matched the known elimination kinetics for histamine, indicating that this system accurately tracks histamine dynamics *in vivo*. Future work will produce new sensors based on this modular platform by replacing the recognition enzyme or replacing both the enzyme and nanosensor as well as directly conjugating the enzymes and nanosensors together. These sensors will enable simultaneous and continuous physiologic measurements for a wide range of analytical targets, and those measurements can establish standards for basal and perturbed health conditions which are difficult to attain with current monitoring techniques.

Supplementary Material

Refer to Web version on PubMed Central for supplementary material.

Acknowledgments

Thank you to J.M. Dubach for design and assembly of the LED light source for *in vivo* imaging. T. Ruckh, J.M. Dubach and M.K. Balaconis provided critical feedback during preparation of the manuscript. This work was supported by DARPA under award number W911NF-11-1-0025 and the National Institute of General Medicine of the National Institutes of Health under award number R01 GM084366.

Funding Sources

This work was supported by DARPA under award number W911NF-11-1-0025, the National Institute of General Medicine of the National Institutes of Health under award number R01 GM084366, and the National Institute Of Biomedical Imaging And Bioengineering of the National Institutes of Health under award number F32EB015270.

ABBREVIATIONS

EnzNS	enzyme nanosensors
O₂NS	oxygen nanosensors
DAO	diamine oxidase
PtTPFPP	Pt(II) meso-Tetra(pentafluorophenyl)porphine

REFERENCES

1. Wilson GS, Hu YB. *Chem. Rev.* 2000; 100:2693–2704. [PubMed: 11749301]
2. Wilson GS, Gifford R. *Biosens. Bioelectron.* 2005; 20:2388–2403. [PubMed: 15854814]
3. Clark LC Jr, Lyons C. *Ann. N. Y. Acad. Sci.* 1962; 102:29–45. [PubMed: 14021529]
4. Cash KJ, Clark HA. *Trends Mol. Med.* 2010; 16:584–593. [PubMed: 20869318]
5. Vaddiraju S, Tomazos I, Burgess DJ, Jain FC, Papadimitrakopoulos F. *Biosens. Bioelectron.* 2010; 25:1553–1565. [PubMed: 20042326]
6. Wang J. *Chem. Rev.* 2008; 108:814–825. [PubMed: 18154363]
7. Shibata H, Heo YJ, Okitsu T, Matsunaga Y, Kawanishi T, Takeuchi S. *Proc. Natl. Acad. Sci. U. S. A.* 2010; 107:17894–17898. [PubMed: 20921374]
8. Heo YJ, Shibata H, Okitsu T, Kawanishi T, Takeuchi S. *Proc. Natl. Acad. Sci. U. S. A.* 2011; 108:13399–13403. [PubMed: 21808049]
9. Billingsley K, Balaconis MK, Dubach JM, Zhang N, Lim E, Francis KP, Clark HA. *Anal. Chem.* 2010; 82:3707–3713. [PubMed: 20355725]
10. Steiner MS, Duerkop A, Wolfbeis OS. *Chem. Soc. Rev.* 2011; 40:4805–4839. [PubMed: 21674076]
11. Xu H, Aylott JW, Kopelman R. *Analyst.* 2002; 127:1471–1477. [PubMed: 12475037]
12. Borisov SM, Klimant I. *Microchim. Acta.* 2009; 164:7–15.
13. Rossi LM, Quach AD, Rosenzweig Z. *Anal. Bioanal. Chem.* 2004; 380:606–613. [PubMed: 15448967]
14. Dubach JM, Balaconis MK, Clark HA. *J. Visualized Exp.* 2011
15. Dubach JM, Zhang N, Lim E, Francis KP, Clark HA. *Integr. Biol.* 2011; 3:142–148.
16. Ruedas-Rama MJ, Hall EAH. *Anal. Chem.* 2010; 82:9043–9049. [PubMed: 20939534]
17. Ozturk G, Feller K-H, Dornbusch K, Timur S, Alp S, Ergun Y. *J. Fluoresc.* 2011; 21:161–167. [PubMed: 20617372]
18. Oberdorster G, Stone V, Donaldson K. *Nanotoxicology.* 2007; 1:2–25.

19. Owens DE, Peppas NA. *Int. J. Pharm.* 2006; 307:93–102. [PubMed: 16303268]
20. Shive MS, Anderson JM. *Adv. Drug Delivery Rev.* 1997; 28:5–24.
21. Jutel M, Watanabe T, Klunker S, Akdis M, Thomet OAR, Malolepszy J, Zak-Nejmark T, Koga R, Kobayashi T, Blaser K, Akdis CA. *Nature*. 2001; 413:420–425. [PubMed: 11574888]
22. Brown RE, Stevens DR, Haas HL. *Prog. Neurobiol. (N. Y.)*. 2001; 63:637–672.
23. Beaven MA, Robinsonwhite A, Roderick NB, Kauffman GL. *Klin. Wochenschr.* 1982; 60:873–881. [PubMed: 6182349]
24. Gustiananda M, Andreoni A, Tabares LC, Tepper AWJW, Fortunato L, Aartsma TJ, Canters GW. *Biosens. Bioelectron.* 2012; 31:419–425. [PubMed: 22152992]
25. Kyriakidis DA, Theodorou MC, Tiligada E. *Front. Biosci., Landmark Ed.* 2012; 17:1108–1119. [PubMed: 22201793]
26. Bourgogne E, Mathy FX, Boucaut D, Boekens H, Laprevote O. *Anal. Bioanal. Chem.* 2012; 402:449–459. [PubMed: 21755269]
27. Guihen E, Ho WL, Hogan AM, O'Connell ML, Leahy MJ, Ramsay B, O'Connor WT, *Chromatogr J. B: Anal. Technol. Biomed. Life Sci.* 2012; 880:119–124.
28. Mou X, Lennartz MR, Loegering DJ, Stenken JA. *Biomaterials.* 2010; 31:4530–4539. [PubMed: 20223515]
29. Bruce C, Weatherstone R, Seaton A, Taylor WH. *Thorax.* 1976; 31:724–729. [PubMed: 1013943]
30. Graham HT, Lowry OH, Wahl N, Priebat MK. *J. Exp. Med.* 1955; 102:307–318. [PubMed: 13252185]
31. Dubach JM, Das S, Rosenzweig A, Clark HA. *Proc. Natl. Acad. Sci. U. S. A.* 2009; 106:16145–16150. [PubMed: 19805271]
32. Dubach JM, Harjes DI, Clark HA. *Nano Lett.* 2007; 7:1827–1831. [PubMed: 17497824]
33. Meier RJ, Schreml S, Wang XD, Landthaler M, Babilas P, Wolfbeis OS. *Angew. Chem., Int. Ed.* 2011; 50:10893–10896.
34. Cywinski PJ, Moro AJ, Stanca SE, Biskup C, Mohr GJ. *Sens. Actuators, B.* 2009; 135:472–477.
35. Petersen LJ, Mosbech H, Skov PS. *J. Allergy Clin. Immunol.* 1996; 97:672–679. [PubMed: 8621853]
36. Pollock I, Murdoch RD, Lessof MH. *Agents Actions.* 1991; 32:359–365. [PubMed: 1907427]
37. Sakurai E, Gunji E, Iizuka Y, Hikichi N, Maeyama K, Watanabe T. *J. Pharmacol. Toxicol. Methods.* 1993; 29:105–109. [PubMed: 7686411]
38. Middleton M, Sarno M, Agarwala SS, Glaspy J, Laurent A, McMasters K, Naredi P, O'Day S, Whitman E, Danson S, Cosford R, Gehlsen K. *J. Clin. Pharmacol.* 2002; 42:774–781. [PubMed: 12092744]
39. Frost M, Meyerhoff ME. *Anal. Chem.* 2006; 78:7370–7377. [PubMed: 17128516]
40. Chang S-Y, Jay T, Munoz J, Kim I, Lee KH. *Analyst.* 2012; 137:2158–2165. [PubMed: 22416270]
41. Ozaydin-Ince G, Dubach JM, Gleason KK, Clark HA. *Proc. Natl. Acad. Sci. U. S. A.* 2011; 108:2656–2661. [PubMed: 21282619]
42. Koren K, Hutter L, Enko B, Pein A, Borisov SM, Klimant I. *Sens. Actuators, B.* 2013; 176:344–350.

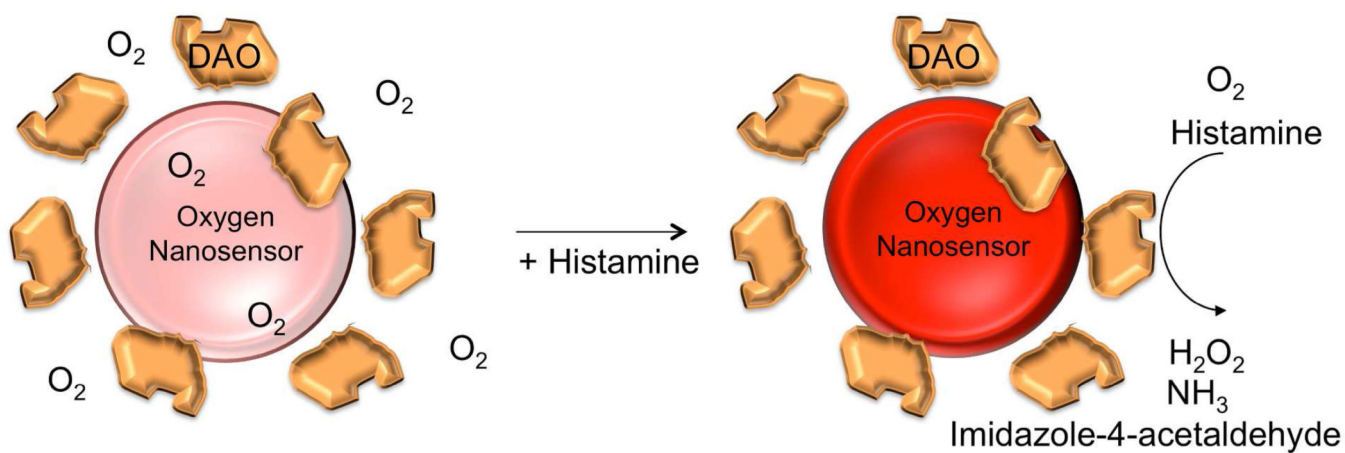


Figure 1.

The Enzyme Nanosensor (EnzNS) system. Enzymatic recognition of histamine by diamine oxidase (DAO) reduces local oxygen concentration, increasing the phosphorescence of oxygen sensitive nanosensors (O₂NS). A decrease in histamine concentration allows oxygen to return, decreasing phosphorescence of the nanosensor. This approach enables detection of histamine for both *in vitro* and *in vivo* applications.

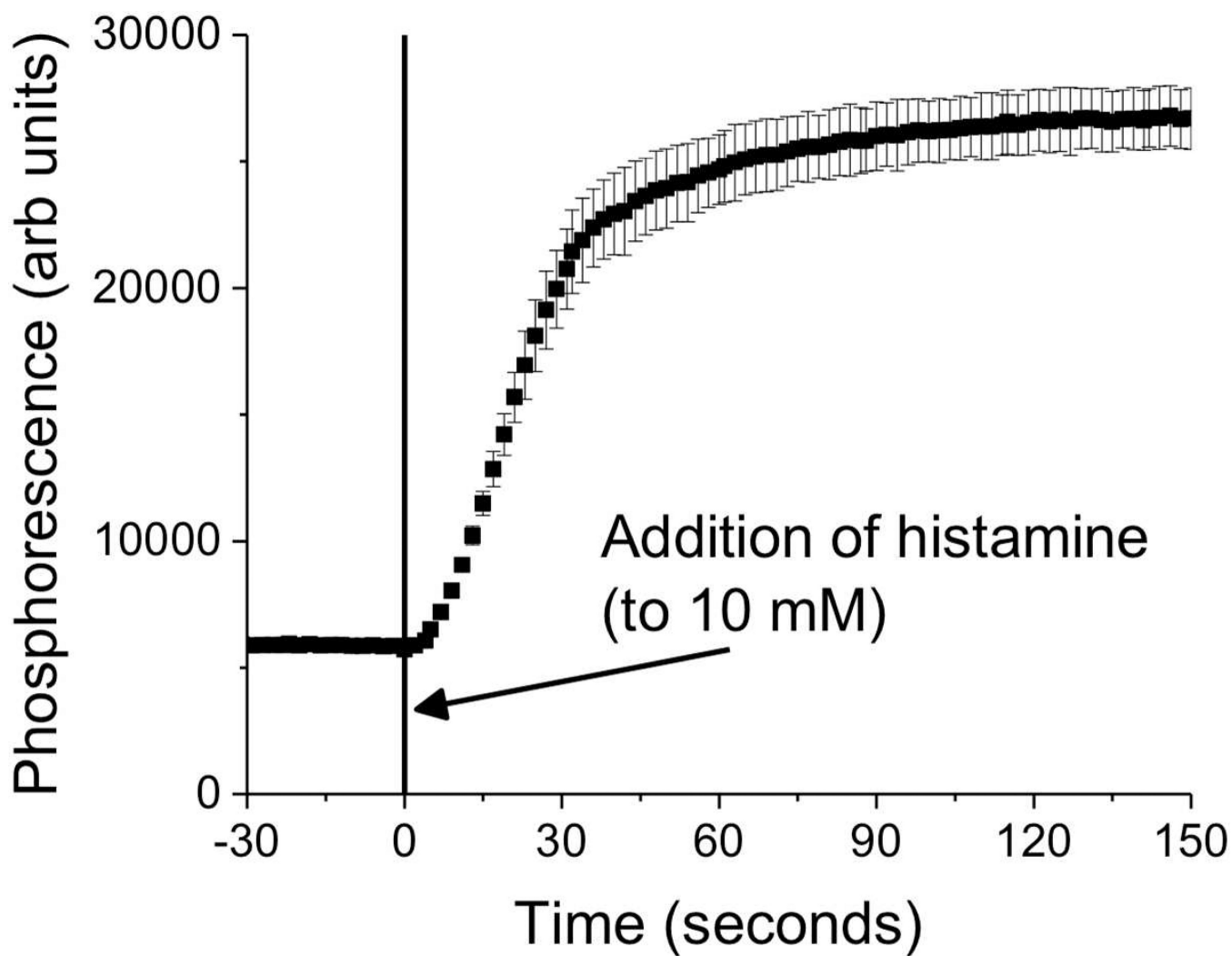


Figure 2. EnzNS response to histamine. Phosphorescence from the nanosensors is low in the absence of histamine. Addition of histamine consumes local oxygen, increasing sensor intensity.

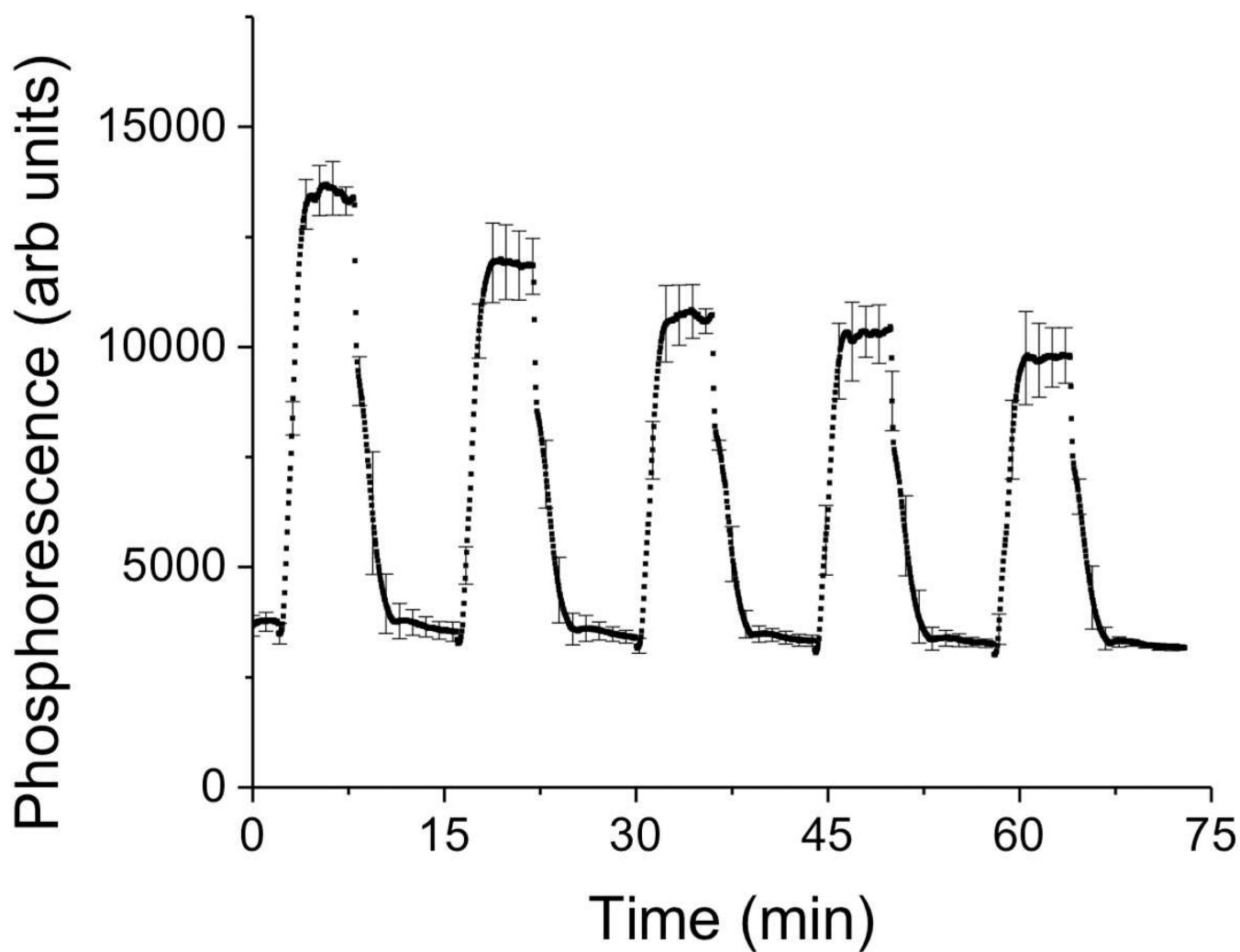


Figure 3. The EnzNS system responds rapidly and reversibly to histamine. After an addition of histamine (to 10 mM) the nanosensors the phosphorescence signal rapidly increases. Flushing the system with fresh buffer reverses the change of the nanosensors, and is repeatable for several cycles of histamine detection.

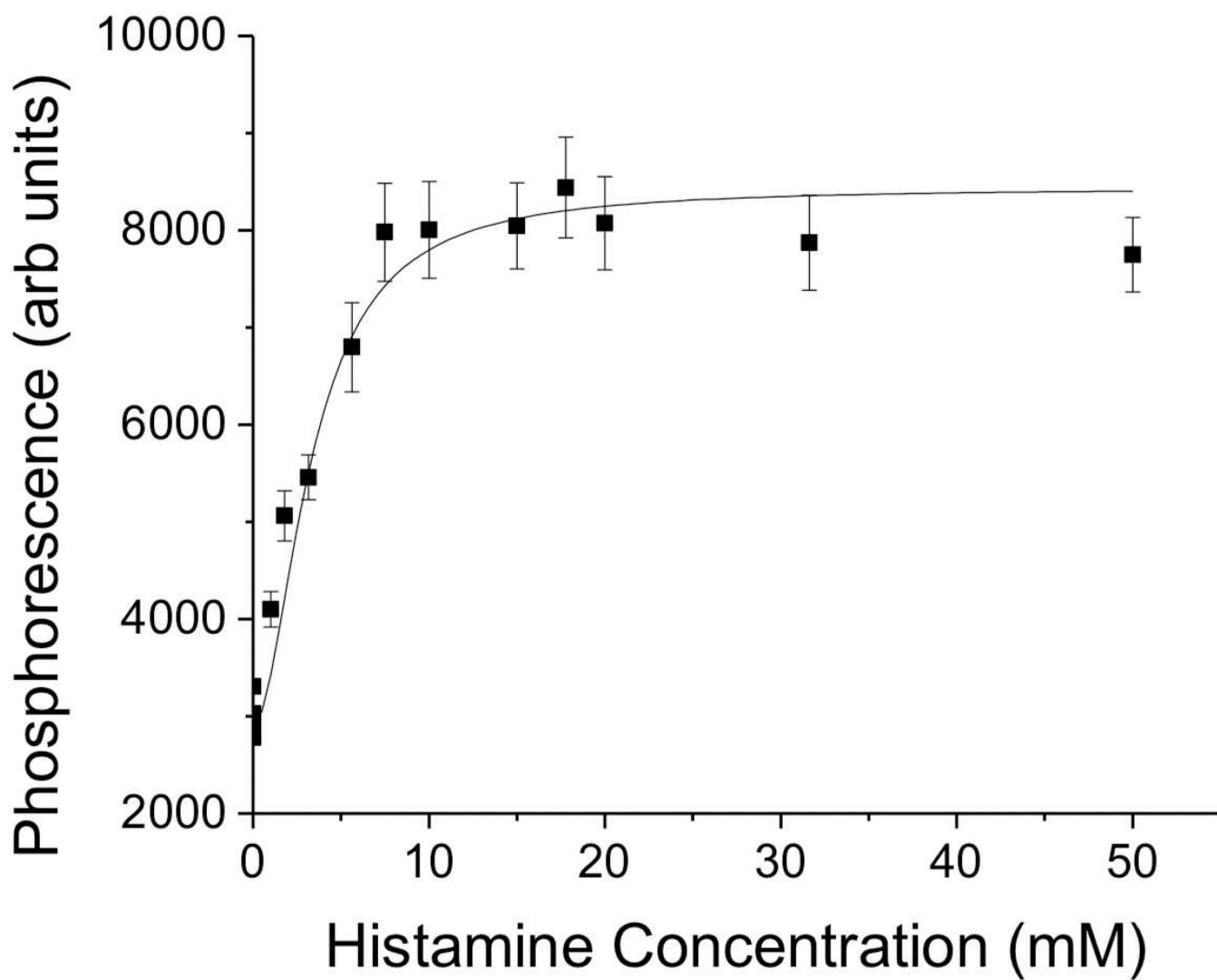


Figure 4. The EnzNS system responds rapidly to histamine concentrations in a dose dependent manner. As histamine concentration is increased the phosphorescence from the nanosensors increases with an apparent binding constant of 3 mM.

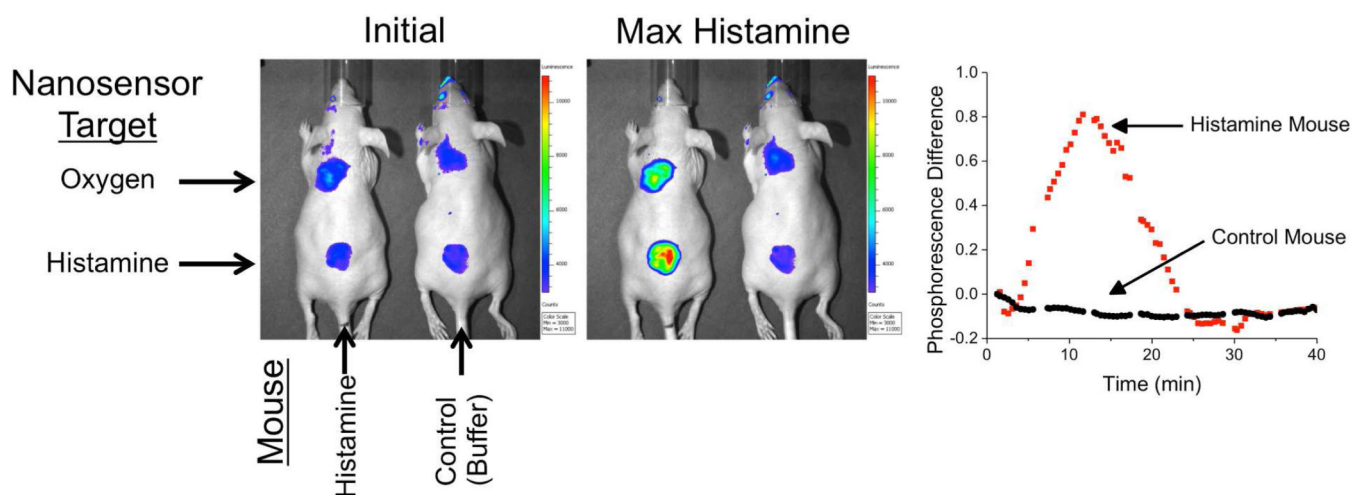


Figure 5.

In vivo experiments demonstrate the ability of intradermal EnzNS to continuously monitor fluctuating histamine levels. As histamine levels increase (via i.p. injection), EnzNS phosphorescence drastically increases (left mouse, bottom injection), while the O₂NS (top injection, controlling for oxygenation effects) shows a much smaller increase. As histamine levels decrease, the EnzNS phosphorescence decreases as well. No signal change is seen from the control mouse (right mouse). The differential signal between the two sensor sites (EnzNS and O₂NS) demonstrates the response of the nanosensors to histamine levels (far right).

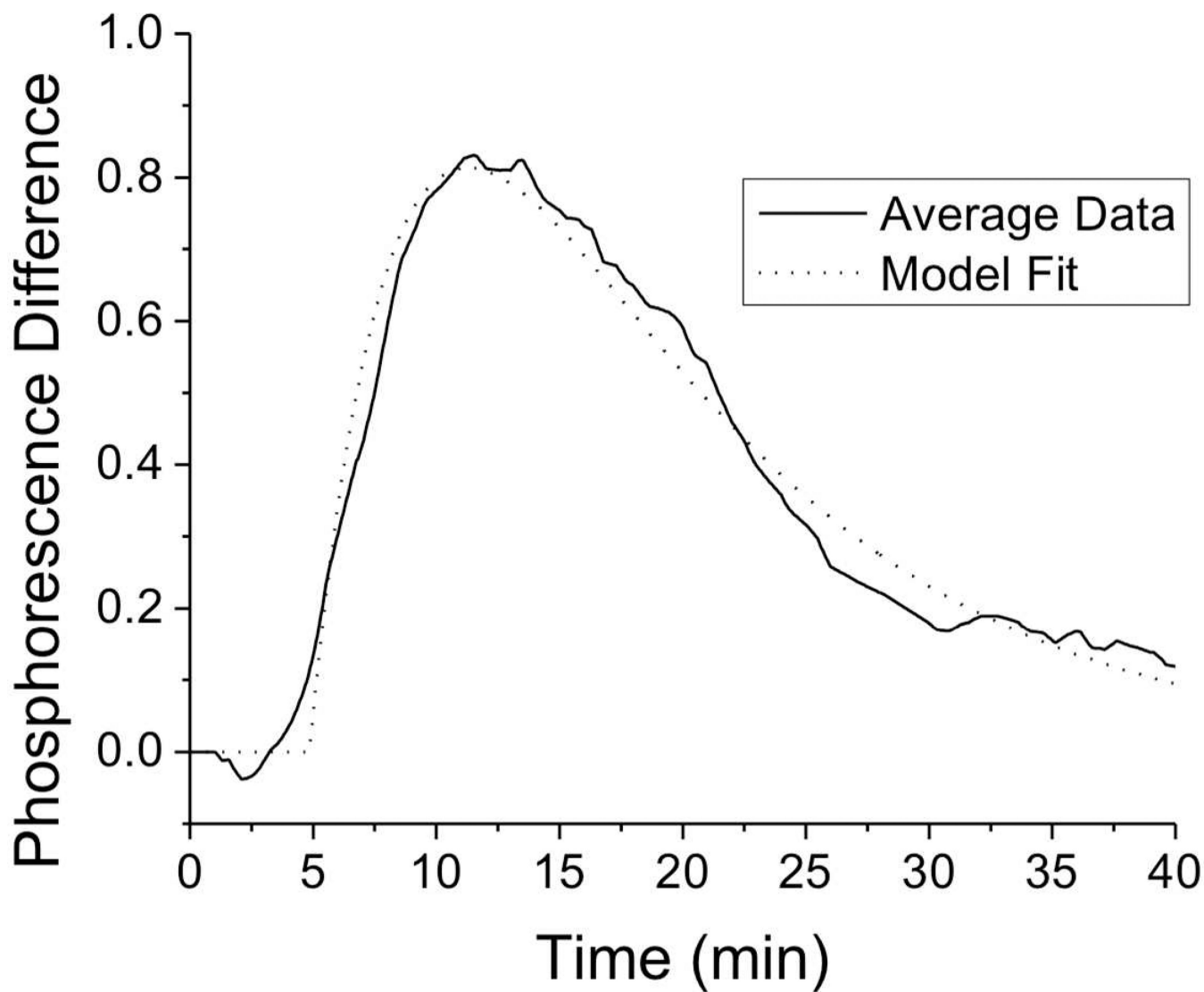


Figure 6.

A one compartment open model fit to the average *in vivo* data. The model parameters yield an elimination half-life of 7.6 minutes, an absorption half-life of 2.8 minutes and a lag time of 4.8 minutes. This data matches well with available literature values³⁵⁻³⁸